

6.2 A selection of FFT applications

Applications of the FFT algorithm are ubiquitous in almost all areas that include computing. The few brief examples here barely start to scratch the surface. The Fourier method for tomographic inversion was described in Section I.1.6 and an example of analyzing a seismogram was quoted at the start of Chapter III.6. This section mentions two more major application areas in Subsections 6.2.1 - 6.2.2 followed by a few numerical uses in Subsections 6.2.3 - 6.2.5.

6.2.1 Image enhancement.

A common task is to sharpen a blurred image - with blurring for example caused by camera motion or bad focusing. As an example, let's consider the sharp image below, and one of its horizontal scan lines:

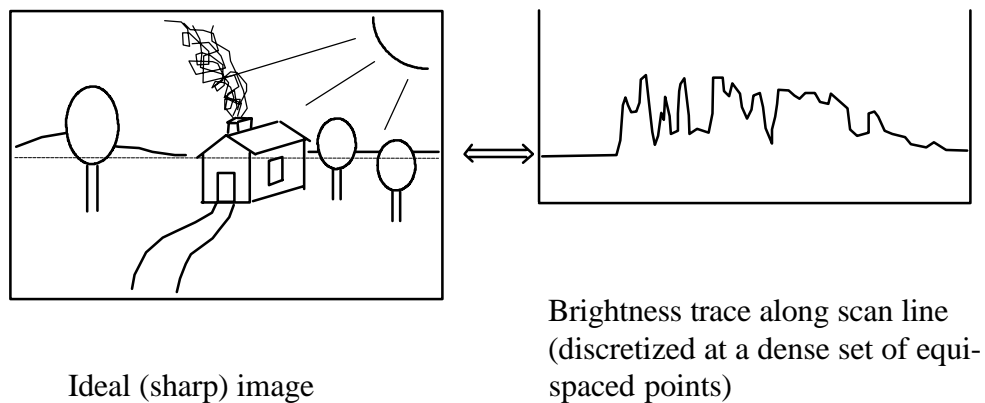


Figure 1. Example of an image and the gray level of a scan line through it.

If the camera was turned sideways during the exposure, the brightness trace would be smeared as if it had been *convolved* with a matrix whose rows are sliding versions of a rectangular pulse function:

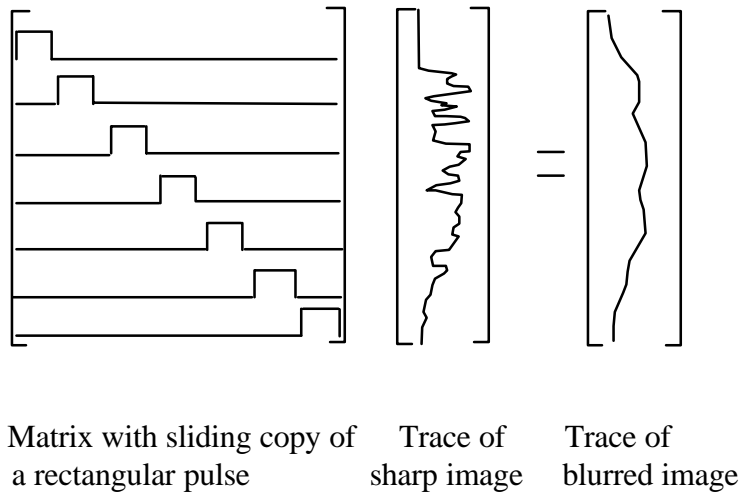


Figure 2. Schematic illustration of how the convolution theorem relates sharp and blurred images.

Comparing with the convolution theorem in equations (I.3.3.7-9), we can identify the vectors x , y , z as follows

z rectangular pulse
 x sharp trace
 y blurred trace

Given any two of these, we quickly find the third through (I.3.3.9) with our interest of course being to recover x with y and z given (or if the perfect z is not known, we can certainly try different z and see which works best). The idea we have here sketched out in 1-D generalizes immediately also to 2-D. For example if the imaging error was bad focusing, the equivalent z would then be a 2-D matrix featuring a circular symmetric Gaussian-type 'hump'.

6.2.2 X-ray Crystallography

The task in X-ray crystallography is to deduce how atoms are arranged within a molecule. If one somehow could

- hold one single molecule isolated and stationary,
- expose it to X-rays that are sufficiently strong that the scattered rays can be detected in all directions, and
- record not only the amplitudes, but also the phases of the scattered rays,

then the atomic arrangement can be calculated immediately from a 3-D Fourier transform (numerically carried out by FFTs - as noted in the introduction to Chapter III.6; this usage pre-dated the 1965 celebrated re-discovery of the FFT algorithm). In practical X-ray crystallography, the first two issues are addressed by applying the technique to a crystal (in which a vast number of the molecules are held in perfect alignment). However, this introduces a new complication in that the X-rays scattered by the different molecules in the crystal lattice interfere with each other, causing canceling the outgoing rays in all but a few directions. We will here discuss just a 2-D model problem to illustrate how come Fourier transforms enter into the picture.

At an arbitrary location \underline{x} , the wave function for an incoming monochromatic X-rays is given by

$$\phi_{inc}(\underline{x}, t) = \phi_0 e^{i(\underline{k}_0 \cdot \underline{x} - \omega t)} \quad . \quad (2)$$

(cf. discussion of wave functions in Section ii4.1). The vector \underline{k}_0 is known as the *wave number*. It points in the direction of wave propagation, and is related to the wavelength λ through $\lambda \|\underline{k}_0\| = 2\pi$. We consider the situation illustrated in Figure 3.

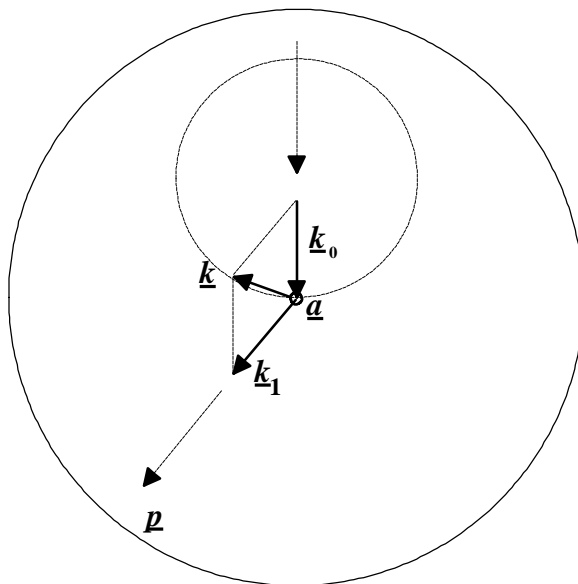


Figure 3. Illustration of an X-ray arriving from above and striking an atom at location \underline{a} and being observed from a location \underline{p} . The figure also illustrates the vectors \underline{k}_0 , \underline{k}_1 and \underline{k} used in the discussion.

The incoming ray (from straight above in Figure 3) strikes an atom located at \underline{a} ; this point is assumed to be very close to the origin in our spatial coordinate system. The scattered wave is recorded at a relatively distant point \underline{p} (e.g. on a sheet of film). The incoming wave at the point \underline{a} is given by (1) with \underline{a} substituted for \underline{x} . The wave function for the scattered wave at the point \underline{p} then becomes

$$\phi_{sc}(\underline{p}, t) = \frac{\phi_0 A}{\|\underline{p}-\underline{a}\|} e^{i(k_0 \cdot \underline{a} - \omega t)} e^{i\|\underline{k}_0\| \cdot \|\underline{p}-\underline{a}\|} \quad , \quad (3)$$

where the scattering coefficient A depends on the type of atom. We have assumed that the amplitude of the scattered wave is the same in all directions, and that it decays proportionally to the traveled distance (the case in 3-D). With minor approximations, this can be rewritten as

$$\phi_{sc}(\underline{p}, t) \approx \frac{\phi_0}{\|\underline{p}\|} e^{i(\|\underline{k}_0\| \cdot \|\underline{p}\| - \omega t)} \cdot [A \cdot e^{-i\mathbf{k} \cdot \underline{a}}] \quad (4)$$

where $\mathbf{k} = \underline{k}_1 - \underline{k}_0$:

Let \underline{k}_1 be a vector of the same length as \underline{k}_0 , but in the direction of $\underline{p} - \underline{a}$ (cf. Figure 3). This vector \underline{k}_1 describes the wave number for the scattered wave received at \underline{p} . It satisfies

$$\frac{\underline{k}_1}{\|\underline{k}_0\|} = \frac{\underline{p}-\underline{a}}{\|\underline{p}-\underline{a}\|} \quad (5)$$

The difference $\underline{p} - \underline{a}$ appears twice in each of the equations (3) and (5). Recalling that $\|\underline{a}\|$ is very small in comparison to $\|\underline{p}\|$ we approximate $\underline{p} - \underline{a}$ with \underline{p} in all these places but in the exponent of (3) (where $\|\underline{k}_0\|$ is large, and the phase information is critical). In that place, we use $\|\underline{p}-\underline{a}\| \approx \|\underline{p}\| - \frac{\underline{k}_1 \cdot \underline{a}}{\|\underline{k}_0\|}$.

To derive this, we note that $\|\underline{p}-\underline{a}\|^2 = \|\underline{p}\|^2 + \|\underline{a}\|^2 - 2\underline{p} \cdot \underline{a}$. Ignoring the quadratic term $\|\underline{a}\|^2$ (but now keeping the linear term $\underline{p} \cdot \underline{a}$) gives $\|\underline{p}-\underline{a}\| \approx \|\underline{p}\|(1 - 2\underline{p} \cdot \underline{a}/\|\underline{p}\|^2)^{1/2} \approx \|\underline{p}\|(1 - \underline{p} \cdot \underline{a}/\|\underline{p}\|^2)$. The result above now follows from (4), when approximated as $\underline{p} \approx \underline{k}_1 \|\underline{p}\|/\|\underline{k}_0\|$.

With these approximations, $\phi_{sc}(\underline{p}, t) \approx \frac{\phi_0 A}{\|\underline{p}\|} e^{i(k_0 \cdot \underline{a} - \omega t)} \cdot e^{i\|\underline{k}_0\| \cdot \|\underline{p}\|} \cdot e^{-i\mathbf{k}_1 \cdot \underline{a}}$, which gives (4).

The purpose in rearranging (3) into (4) is that all the quantities associated with the atom (scattering coefficient A and position \underline{a}) appear now only in the last bracket.

Instead of one atom only, we consider next the whole group of N atoms which form the molecule. These are located at nearby positions \underline{a}_n and have individual scattering coefficients A_n , $n = 1, 2, \dots, N$. Still assuming that secondary scatterings can be neglected, the wave received at \underline{p} becomes

$$\phi_{sc}(\underline{p}, t) \approx \frac{\phi_0}{\|\underline{p}\|} e^{i(\|\underline{k}_0\| \cdot \|\underline{p}\| - \omega t)} \cdot \left[\sum_{n=1}^N A_n \cdot e^{-i\mathbf{k} \cdot \underline{a}_n} \right] \quad (6)$$

By recording ϕ_{sc} at all different positions \underline{p} around the crystal, we have in fact recorded

$$\hat{A}(\mathbf{k}) = \sum_{n=1}^N A_n \cdot e^{-i\mathbf{k} \cdot \underline{a}_n} \quad (7)$$

around the dotted circle in Figure 3. Atoms are not quite point-like. It is better to think of A as a continuous function of position, i.e. to replace (7) by

$$\hat{A}(\underline{k}) = \iint A(\underline{x}) e^{-i\underline{k}\cdot\underline{x}} d\underline{x} = \iint A(x_1, x_2) e^{-i(k_1x_1+k_2x_2)} dx_1 dx_2 . \quad (8)$$

We have arrived precisely at a standard 2-D Fourier transform. Therefore, it is more natural to write $\underline{k} = (\omega_1, \omega_2)$ and to plot the physical $\underline{x} = (x_1, x_2)$ and Fourier $\underline{k} = (\omega_1, \omega_2)$ spaces beside each other (rather than superimposed as in Figure 3):

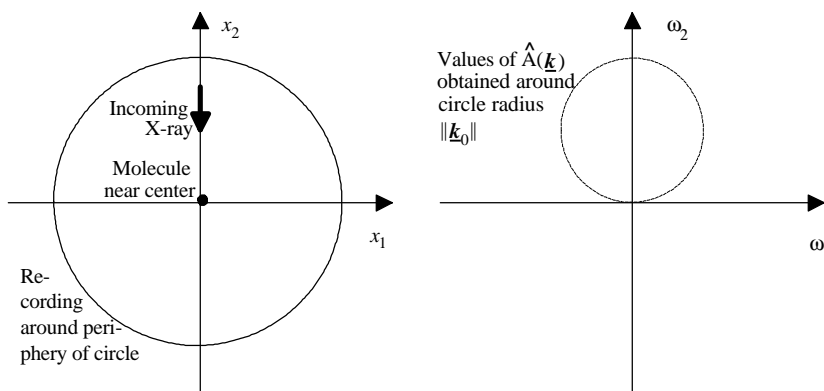


Figure 4. Illustration of physical set-up and the circle in Fourier $\underline{k} = (\omega_1, \omega_2)$ - space around which we get data for $\hat{A}(\omega_1, \omega_2)$.

Like in the FT method for tomography, we next appeal to the theorem that rotating a function rotates its Fourier transform the same angle. Rotating the molecule around the center in the $\underline{x} = (x_1, x_2)$ -plane rotates the dashed circle in the $\underline{k} = (\omega_1, \omega_2)$ -plane around the center in that plane. This allows us to obtain data for $\hat{A}(\omega_1, \omega_2)$ throughout the interior of the domain $\|\underline{k}\| \leq 2 \|\underline{k}_0\|$. According to (8) it remains only to do a 2-D Fourier transform to obtain the function $A(x_1, x_2)$ describing the positions and types of the atoms in the molecule.

For pioneering work in the field of X-ray scattering by crystals, the Nobel Prize in Physics for 1914 was awarded to M. von Laue and for 1915 to W.H. Bragg and W.L. Bragg (father and son; W.L. Bragg at age 25 the youngest Nobel Prize winner in history). These initial efforts were of great significance in establishing the lattice arrangement of atoms in crystals, as well as the wave nature of X-rays. Seventy years later, the 1985 Nobel Prize in Chemistry was awarded to H. Hauptman and J. Karle for their solution to the phase problem:

Current recording techniques for $\phi_{sc}(p, t)$ provides only $|\hat{A}(\underline{k})|$, but the phase information of the complex quantity $\hat{A}(\underline{k})$ is lost. One idea to compensate for this is to try to exploit that $A(\underline{x})$ should be a strictly

non-negative function; another is to incorporate certain probabilistic ideas. Hauptman's and Karle's work along these lines (in the early 1950's when both were working at the US Naval Research Laboratory, in Washington DC) made 'direct methods' near-routine for molecules of up to around 100 atoms.

Numerous Nobel Prizes in Chemistry and Medicine have been awarded for work in which X-ray crystallography has been a major tool. They include L. Pauling (Ch., 1954), M. Perutz and J. Kendrew (Ch., 1962), F. Crick, J. Watson and M. Wilkins (Med., 1962 - the discovery of the structure of DNA depended critically on X-ray work by R. Franklin), D. Hodgkin (Ch., 1964), O. Hassle and D. Barton (Ch., 1969), W. Lipscomb (Ch., 1976) and A. Klug (Ch., 1982).

...

(list OK only up to 1985 - check more recently!)

6.2.3 Numerical Chebyshev expansion of a function.

Any continuous function on, say, $[-1,1]$ can be approximated as closely as we want by a polynomial. A bad way to do this is to interpolate the function at increasingly many equi-spaced points - the resulting polynomial will usually oscillate violently near the ends of the interval (known as the Runge phenomenon). By putting the interpolation nodes denser towards the edges, oscillations can be perfectly suppressed. The choice

$$x_k = -\cos \frac{\pi k}{N} \quad , \quad k = 0, 1, 2, \dots, N$$

is particularly effective; convergence to $f(x)$ is usually very rapid as N increases. The Fast Cosine Transform (cf.) is in this case much faster than using Lagrange's or Newton's interpolation formulas. For this, we need to consider the *Chebyshev polynomials*

$$\begin{aligned} T_0(x) &= \cos(0 \arccos x) &= 1 & , \\ T_1(x) &= \cos(1 \arccos x) &= x & , \\ T_2(x) &= \cos(2 \arccos x) &= 2x^2 - 1 & , \\ T_3(x) &= \cos(3 \arccos x) &= 4x^3 - 3x & , \\ & \cdot & & \\ T_n(x) &= \cos(n \arccos x) &= 2^{n-1} x^n - \dots & . \end{aligned}$$

$T_n(x)$ is clearly a polynomial of degree n for $n = 0$ and $n = 1$; for higher n this follows for ex. from the three-term recursion formula $T_{n+1}(x) = 2x T_n(x) - T_{n-1}(x)$ (a consequence of the trigonometric identity $\cos((n+1)\alpha) + \cos((n-1)\alpha) = 2 \cos \alpha \cos n\alpha$ if we let $\alpha = \arccos x$, i.e. $\cos \alpha = x$).

Making the polynomial

$$p_n(x) = \sum_{v=0}^n \alpha_v T_v(x)$$

agree with $f(x)$ at the nodes $x_k = -\cos \frac{\pi k}{n}$ amounts to finding values of α_v such that

$$\sum_{v=0}^n \alpha_v T_v(x_k) = f(x_k) \quad .$$

With $T_v(x_k) = \cos(v \arccos(-\cos \frac{\pi k}{n})) = \cos v \frac{\pi k}{n}$, this becomes

$$\sum_{v=0}^n \alpha_v \cos v \frac{\pi k}{n} = f(x_k) \quad (k = 0, 1, \dots, n) .$$

Therefore, the desired expansion coefficients are obtained as the output of an FCT, applied to the function values $f(x_k)$, $k = 0, 1, \dots, n$.

If one wants, one can re-sort the expansion $\sum_{v=0}^n \alpha_v T_v(x)$ into the more usual form $\sum_{v=0}^n \beta_v x^v$, but there is usually little reason to do that. Thanks to many formulas relating to the Chebyshev polynomials, they are fast to evaluate and easy to manipulate (to differentiate etc.) A notable advantage with them is

that for any $f(x)$ continuous on $[-1,1]$, there is a unique expansion $f(x) = \sum_{v=0}^{\infty} \alpha_v T_v(x)$ for which truncations offer excellent approximations. The situation for power series is much less attractive; for $f(x) = \sum_{v=0}^{\infty} \beta_v x^v$ to hold, it is not even sufficient that $f(x)$ is infinitely many times differentiable over $[-1,1]$. And even when there is a convergent power series expansion, truncations are usually reasonably accurate only near $x = 0$.

6.2.4 Numerical computation of Taylor coefficients

Although this is not a task that is particularly often needed, it is interesting to note that again, the FFT makes this not only possible, but also very effective. If a function $f(x)$ can be computed numerically only for real arguments x (the most common situation), we can do little better than applying the finite difference approximations from Section II.2.2-4. Especially approximations for high derivatives become very sensitive to small errors in function values.

For example, if we approximate a fourth derivative by

$$f^{(4)}(x) = \frac{f(x-2h) - 4f(x-h) + 6f(x) - 4f(x+h) + f(x+2h)}{h^4} + O(h^2) \quad (8)$$

(cf. Table 1 in Section II.2.4), we need h to be small so that the truncation error $O(h^2)$ is small. But then, the $O(h^4)$ in the denominator is far smaller still, causing errors in function values to get greatly magnified. Another way to view the problem: If the fourth derivative is an $O(1)$ - quantity, and the numerator is very small, the numerator must be equally small. This means that the numerator must have been obtained through the subtraction of almost equally big numbers - the ONLY way to lose a large number of significant digits in floating point arithmetic.

If $f(x)$ is an analytic function

i.e. once differentiable in the sense that $f'(x) = \lim_{h \rightarrow 0} \frac{f(x+h)-f(x)}{h}$ exists for all complex $h \rightarrow 0$ - it will then automatically be infinitely many times differentiable,

then $f(x)$ can be Taylor expanded around x :

$$f(x+h) = f(x) + h \frac{f'(x)}{1!} + h^2 \frac{f''(x)}{2!} + h^3 \frac{f'''(x)}{3!} + \dots \quad (9)$$

If we sample f not at equi-spaced points on the real axis (such as in (8)) but instead around a circle $z = x + h$ with $h = \alpha e^{i\theta}$, $0 \leq \theta \leq 2\pi$, then (9) becomes

$$f(x + \alpha e^{i\theta}) = f(x) + \frac{\alpha f'(x)}{1!} e^{i\theta} + \frac{\alpha^2 f''(x)}{2!} e^{2i\theta} + \frac{\alpha^3 f'''(x)}{3!} e^{3i\theta} + \dots$$

The RHS is a Fourier Series; the LHS can be computed for equi-spaced values of θ . By the FFT algorithm, we can quickly approximate the Fourier coefficients $\alpha^k f^{(k)}(x)/k!$, i.e. the derivatives of $f(x)$. The constant α is a free parameter. Fornberg (1981a,b) describe in some detail how results for a few values of α can be combined to effectively compute the high derivatives.

6.2.5 Multiplication of Large Polynomials

The product of

$$\begin{aligned} p_1(x) &= a_0 + a_1x + a_2x^2 + \dots + a_Nx^N \quad \text{and} \\ p_2(x) &= b_0 + b_1x + b_2x^2 + \dots + b_Nx^N \end{aligned}$$

is

$$\begin{aligned} p_1(x) \cdot p_2(x) &= 1 \cdot \{a_0b_0\} + \\ &\quad x \cdot \{a_1b_0 + a_0b_1\} + \\ &\quad x^2 \cdot \{a_2b_0 + a_1b_1 + a_0b_2\} + \\ &\quad \cdot \\ &\quad \cdot \\ &\quad x^N \cdot \{a_Nb_0 + a_{N-1}b_1 + a_{N-2}b_2 + \dots + a_1b_{N-1} + a_0b_N\} + \\ &\quad \cdot \\ &\quad \cdot \\ &\quad x^{2N-1} \cdot \{a_Nb_{N-1} + a_{N-1}b_N\} + \\ &\quad x^{2N} \cdot \{a_Nb_N\} \\ &= c_0 + c_1x + c_2x^2 + \dots + c_{2N}x^{2N}. \end{aligned}$$

This can be written in matrix / vector form as

$$\begin{bmatrix} a_0 & 0 & \dots & \dots & 0 & a_N & \dots & a_2 & a_1 \\ a_1 & a_0 & 0 & \dots & \dots & 0 & a_N & \dots & a_2 \\ a_2 & a_1 & a_0 & 0 & \dots & \dots & 0 & a_N & \dots \\ \dots & a_2 & a_1 & a_0 & 0 & \ddots & \ddots & 0 & a_N \\ \ddots & \ddots & \ddots & \ddots & \ddots & \ddots & \ddots & \ddots & \ddots \\ 0 & a_N & \dots & a_2 & a_1 & a_0 & 0 & \ddots & \ddots \\ \dots & 0 & a_N & \dots & a_2 & a_1 & a_0 & 0 & \dots \\ \dots & \dots & 0 & a_N & \dots & a_2 & a_1 & a_0 & 0 \\ 0 & \dots & \dots & 0 & a_N & \dots & a_2 & a_1 & a_0 \end{bmatrix} \begin{bmatrix} b_0 \\ b_1 \\ b_2 \\ \vdots \\ b_N \\ 0 \\ \vdots \\ \vdots \\ 0 \\ c_{2N} \end{bmatrix} = \begin{bmatrix} c_0 \\ c_1 \\ c_2 \\ \vdots \\ \vdots \\ \vdots \\ \vdots \\ \vdots \\ \vdots \\ \vdots \\ c_{2N} \end{bmatrix}$$

where we have introduced N zeros following the $N+1$ elements of the a - and b -vectors (we can pad with additional zeros if we want to make the vector sizes a power of two or something else that is fast for the FFT). This matrix-vector product is of the form that was shown in equation II.3.3 (8) to allow a fast evaluation with the discrete convolution theorem. With FFTs, this costs $O(N \log N)$ operations (rather than $O(N^2)$ if multiplied directly).

